Platinum Dioxide Cation: Easy to Generate Experimentally but Difficult to Describe Theoretically

Mark Brönstrup, Detlef Schröder,* Ilona Kretzschmar, Helmut Schwarz,*,† and Jeremy N. Harvey*

Contribution from the Institut für Organische Chemie, Technischen Universität Berlin, Strasse des 17. Juni 135, D-10623 Berlin, Germany, and the School of Chemistry, University of Bristol, Cantock's Close Bristol BS8 1TS, U.K.

Received August 22, 2000

Abstract: A formal platinum(V) dioxide cation $[Pt,O_2]^+$ can be generated in the gas phase by successive oxidation of Pt^+ with N_2O. The ion's reactivity is in keeping with the dioxide structure $OPtO^+$, rather than with $[Pt,O_2]^+$ isomers having intact O−O bonds, e.g., the dioxygen complex $Pt(O_2)^+$ and peroxo species $PtOO^+$. Inter alia due to the high ionization energy of the neutral counterpart (11.2 eV), the $[Pt,O_2]^+$ cation is a rather aggressive reagent toward oxidizable neutrals. $[Pt,O_2]^+$ is even capable of activating inert substrates such as H_2, CO, and CH_4. Further, a sequence for the catalytic conversion $CO + N_2O \rightarrow CO_2 + N_2$ is described with a turnover number of >100 for the catalytically active species PtO_n^+ ($n = 0-2$). As a consequence of the high reactivity, however, the observed selectivities with most substrates are rather poor. For example, the reaction of PtO_2^+ with ethane gives rise to 10 different product channels. In an attempt to analyze the structural features and different minima of the $[Pt,O_2]^+$ system, extensive ab initio studies are performed. While correlated ab initio methods describe the system reasonably well, density functional theory turns out to be much less accurate in terms of both structural and energetic descriptions.

Ever since Döbereiners lighter, elemental platinum has been known to catalyze combustion effectively. Ignition of a flame requires activation of either the combustible material or the oxidant; considering the various applications of platinum in catalysis, this particular metal is obviously able to fulfill both tasks simultaneously. In the gas phase, for example, bare Pt^+ cations are capable of activating methane[1,2] to afford a carbene complex $PtCH_2^+$, which can subsequently be oxidized by molecular oxygen to regenerate Pt^+, thereby giving rise to a catalytic sequence.[3−5]

Here, we describe gas-phase reactions of the $[Pt,O_2]^+$ cation[6] with simple inorganic substrates and hydrocarbons as model systems for oxidation catalysis at a molecular level.[7] Deliberately, we use the notation $[Pt,O_2]^+$ because the ion generated experimentally may correspond to a dioxide $OPtO^+$, a peroxide $PtOO^+$, or even a dioxygen complex $Pt(O_2)^+$. The structural dichotomy of $[M,O_2]^+$ species is far from being only semantic because the properties and in particular the reactivities of the various isomers may differ significantly.[8] To clarify the ion's structure and to probe the reactivity, we investigate $[Pt,O_2]^+$ both experimentally, using Fourier Transform ion-cyclotron resonance (FTICR) mass spectrometry, and computationally, using a variety of methods.

Experimental and Theoretical Methods

Ion/molecule reactions were examined with a Spectrospin CMS 47X FTICR-MS equipped with an external ion source as described elsewhere.[9,10] In brief, Pt^+ was generated by laser ablation of a platinum target using a Nd:YAG laser operating at 1064 nm. Using a series of potentials and ion lenses, the ions were transferred to the ICR cell which is positioned in the bore of a 7.05 T superconducting magnet. Mass-selected $^{195}Pt^+$ was then converted to $[Pt,O_2]^+$ by reaction with pulsed-in N_2O.[11] After subsequent mass selection of $[^{195}Pt,^{16}O_2]^+$, the ion's reactivity was studied by introducing the neutral reactants via leak valves. The experimental second-order rate constants were evaluated assuming the pseudo-first-order kinetic approximation after calibration of the measured pressure and acknowledgment of the ion gauge sensitivities.[12] The error of the absolute rate constants is ±30%, and the ion temperature is assumed as 298 K.[13]

Density functional computations were performed using the standard B3LYP and BP86 functionals as implemented in the Gaussian 98

† Technische Universität Berlin.

(1) Irikura, K. K.; Beauchamp, J. L. *J. Am. Chem. Soc.* **1991**, *113*, 2769.
(2) Irikura, K. K.; Beauchamp, J. L. *J. Phys. Chem.* **1991**, *95*, 8344.
(3) Wesendrup, R.; Schröder, D.; Schwarz, H. *Angew. Chem.* **1994**, *106*, 1232; *Angew. Chem., Int. Ed. Engl.* **1994**, *33*, 1174.
(4) Heinemann, C.; Wesendrup, R.; Schwarz, H. *Chem. Phys. Lett.* **1995**, *239*, 75.
(5) Pavlov, M.; Blomberg, M. R. A.; Siegbahn, P. E. M.; Wesendrup, R.; Heinemann, C.; Schwarz, H. *J. Phys. Chem. A* **1997**, *101*, 1567.
(6) Brönstrup, M. Organometallic Ion Chemistry of Iron and Platinum in the Gas Phase; Dissertation, TU Berlin D83, Shaker, Aachen, 2000.
(7) (a) Schröder, D.; Schwarz, H. *Angew. Chem.* **1995**, *107*, 2126; *Angew. Chem., Int. Ed. Engl.* **1995**, *34*, 1973. (b) Schröder, D.; Shaik, S.; Schwarz, H. In *Structure and Bonding*; Vol. 97, *Metal−Oxo and Metal−Peroxo Species in Catalytic Oxidations*; Meunier, B., Ed.; Springer: Berlin, 2000; p 91.
(8) (a) Schröder, D.; Fiedler, A.; Schwarz, J.; Schwarz, H. *Inorg. Chem.* **1994**, *33*, 5094. (b) Schröder, D.; Fiedler, A.; Herrmann, W. A.; Schwarz, H. *Angew. Chem.* **1995**, *107*, 2714; *Angew. Chem., Int. Ed. Engl.* **1995**, *34*, 2517. (c) Fiedler, A.; Kretzschmar, I.; Schröder, D.; Schwarz, H. *J. Am. Chem. Soc.* **1996**, *118*, 9941. (d) Schröder, D.; Jackson, P.; Schwarz, H. *Eur. J. Inorg. Chem.* **2000**, 1171. (e) Jackson, P.; Harvey, J. N.; Schröder, D.; Schwarz, H. *Int. J. Mass Spectrom.* In press.
(9) Eller, K.; Schwarz, H. *Int. J. Mass Spectrom. Ion Processes* **1989**, *93*, 243.
(10) Eller, K.; Zummack, W.; Schwarz, H. *J. Am. Chem. Soc.* **1990**, *112*, 621.
(11) Brönstrup, M.; Schröder, D.; Schwarz, H. *Organometallics* **1999**, *18*, 1939.
(12) More complex reaction kinetics were modeled with the user-based program *ICR Kinetics 3.1.0* written by U. Mazurek and H. Schwarz; available upon request from the following: ulf@www.chem.tu-berlin.de.

10.1021/ja003138q CCC: $20.00
Published on Web 12/08/2000

program package.[14] At the indicated levels of theory, full geometry optimizations and frequency calculations were performed to verify the nature of the minima and to evaluate zero-point energies. Unrestricted wave functions were used for all open-shell species. The notation BS I refers to the use of the standard LANL2DZ effective core potential (ECP) together with the associated (8s6p3d)/[3s3p2d] double-ζ basis to describe the 5s, 5p, 5d, and 6s electrons on platinum and the 6-31+G* basis on oxygen. BS II and BS III both use the more flexible triple-ζ 6-311+G(2d) basis on oxygen. For platinum, BS II uses the LANL2DZ ECP as in BS I, but with an expanded (8s6p4d3f)/[4s4p4d2f] basis on Pt,[15] obtained by decontracting the outermost contracted s, p, and d primitive of the LANL2DZ standard contraction, adding one diffuse d function (α = 0.137) and 3 f primitives (α = 1.144943, contraction coefficient 0.5458; α = 0.466, contraction coefficient 0.4506; α = 0.1897, uncontracted). In BS III, platinum is instead described with the Stuttgart SDD ECP[16] and the associated basis implemented in Gaussian with one *f* function (α = 0.7) added.

Multireference second-order perturbation theory (MR-PT2) computations were performed using the program packages GAMESS-USA[17] for multiconfigurational quasidegenerate perturbation theory (MC-QDPT)[18] and MOLPRO 2000[19] for complete active space + perturbation theory (CASPT2) using the modified g4 operator.[20] The active space included the 2s and 2p orbitals and electrons of oxygen and the 5d shell of platinum, which means, for example, 21 electrons in 13 orbitals for the $[Pt,O_2]^+$ species. Test calculations were performed on Pt^+, PtO^+, and $^2OPtO^+$ at the CASSCF and CASPT2 levels, including the formally Pt 6s orbital in the active space. Bond energies and lengths (for PtO^+) were not significantly changed. Given these observations and the fact that the expanded active space led to a substantial increase in the computational expense, this approach was not pursued in the $[Pt,O_2]^+$ system. All orbitals were fully optimized during the MCSCF computations, but for the perturbation treatment, the Pt Pt 5s and 5p and O 1s electrons, which are much lower in energy than the valence electrons, were kept frozen as is usual for core electrons. The geometry of all species was optimized at the MC-QDPT level of theory in GAMESS using the TRUDGE method based on numerical gradients.[17] The geometries of the two dioxo spin states of $OPtO^+$ were assumed to have at least C_{2v} symmetry. Optimization of the C_s-symmetric superoxide $PtOO^+$ failed using the TRUDGE routine, and it was instead performed manually to within ±0.01 Å and ±2°. Single-point computations indicated that all states with wave functions of different symmetries from those discussed here lie significantly higher in energy, so they were not further investigated. BS IV uses the standard SBKJ ECP on Pt,[21] together with the associated (7s7p5d)/[4s4p3d] basis set to describe the 5s, 5p, 5d, and 6s electrons, with one added f function (α = 0.7), and the DZV(d) basis set on oxygen. BS V and VI are based on the same Stuttgart ECP as above in BS III (ECP60MWB in MOLPRO). BS V uses the unmodified built-in (8s7p6d)/[6s5p3d] basis set, to which one *f* function (α = 0.7) is added, and the standard cc-pVDZ basis on oxygen. In BS VI, the cc-pVTZ basis is used instead on oxygen, and for platinum, the outermost contracted d primitive is removed from the contraction, the single f function is replaced by two even-tempered ones (ratio = 2.8, center = 0.8), and a single g function (α = 1.1) is added, to yield a (8s7p6d2f1g)/[6s5p4d2d1g] basis. The platinum polarization functions used were energy optimized at the CI level.

Results and Discussion

The thermochemistry of the $[Pt,O_2]^+$ system has been established reasonably well by Knudsen-cell methods.[22,23] The Lias compendium[24] lists heats of formation (at 298 K) of $\Delta_f H°(PtO) = 101 \pm 5$ kcal/mol[25] and $\Delta_f H°(PtO_2) = 41 \pm 3$ kcal/mol in conjunction with the ionization energies $IE(PtO) = 10.1 \pm 0.3$ eV and $IE(PtO_2) = 11.2 \pm 0.3$ eV. Combined with supplementary data for Pt, O, and O_2, these values suggest the bond-dissociation energies $D(Pt^+-O) = 60 \pm 9$ kcal/mol and $D(OPt^+-O) = 95 \pm 8$ kcal/mol, respectively. Recent and more precise, direct determinations by ion-beam techniques give $D_0(Pt^+-O) = 75.2 \pm 1.2$ kcal/mol and $D_0(OPt^+-O) = 71.0 \pm 1.2$ kcal/mol.[26] The sum $D(Pt^+-O) + D(OPt^+-O) = 146$ kcal/mol also agrees well with the Knudsen-cell data (155 kcal/mol).[27] For the evaluation of the thermochemical features of the $[Pt,O_2]^+$ system described further below, we use the values of Zhang and Armentrout[26] as anchors.

Mass Spectrometric Experiments. Under gas-phase conditions, the generation of the $[Pt,O_2]^+$ cation from atomic Pt^+ can proceed in a straightforward manner according to reactions 1 and 2 using nitrous oxide.[6,11]

$$Pt^+ + N_2O \rightarrow PtO^+ + N_2 \quad (1)$$

$$PtO^+ + N_2O \rightarrow [Pt,O_2]^+ + N_2 \quad (2)$$

The first O-atom transfer to platinum is about three times slower than the second ($k_1 = 0.7 \times 10^{-10}$ cm^3 molecules^{-1} s^{-1} vs $k_2 = 1.9 \times 10^{-10}$ cm^3 molecules^{-1} s^{-1}). The absence of side or subsequent reactions upon treatment of Pt^+ with N_2O in the gas phase allows for a clean and facile production of $[Pt,O_2]^+$. To obtain some insight into the ion's properties, the reactivity of the mass-selected $[Pt,O_2]^+$ species toward various neutral reagents is examined.

The first experiment to be discussed is isotopic exchange with ^{18}O compounds. Upon treatment of $[Pt,^{16}O_2]^+$ with $H_2{}^{18}O$, rapid $^{16}O/^{18}O$ exchanges to yield $[Pt,^{16}O,^{18}O]^+$ and then $[Pt,^{18}O_2]^+$

(13) Schröder, D.; Schwarz, H.; Clemmer, D. E.; Chen, Y.-M.; Armentrout, P. B.; Baranov, V. I.; Böhme, D. K. *Int. J. Mass Spectrom. Ion Processes* **1997**, *161*, 177.

(14) Frisch, M. J.; Trucks, G. W.; Schlegel, H. B.; Scuseria, G. E.; Robb, M. A.; Cheeseman, J. R.; Zakrzewski, V. G.; Montgomery, J. A., Jr.; Stratmann, R. E.; Burant, J. C.; Dapprich, S.; Millam, J. M.; Daniels, A. D.; Kudin, K. N.; Strain, M. C.; Farkas, O.; Tomasi, J.; Barone, V.; Cossi, M.; Cammi, R.; Mennucci, B.; Pomelli, C.; Adamo, C.; Clifford, S.; Ochterski, J.; Petersson, G. A.; Ayala, P. Y.; Cui, Q.; Morokuma, K.; Malick, D. K.; Rabuck, A. D.; Raghavachari, K.; Foresman, J. B.; Cioslowski, J.; Ortiz, J. V.; Stefanov, B. B.; Liu, G.; Liashenko, A.; Piskorz, P.; Komaromi, I.; Gomperts, R.; Martin, R. L.; Fox, D. J.; Keith, T.; Al-Laham, M. A.; Peng, C. Y.; Nanayakkara, A.; Gonzalez, C.; Challacombe, M.; Gill, P. M. W.; Johnson, B. G.; Chen, W.; Wong, M. W.; Andres, J. L.; Head-Gordon, M.; Replogle, E. S.; Pople, J. A. *Gaussian 98*, revision A.7; Gaussian, Inc.: Pittsburgh, PA, 1998.

(15) The basis set was kindly provided to us by P. E. M. Siegbahn.

(16) Andrae, D.; Häussermann, U.; Dolg, M.; Stoll, H.; Preuss, H. *Theor. Chim. Acta* **1990**, *77*, 123.

(17) GAMESS-USA (version of 1 December 1, 1998): Schmidt, M. W.; Baldridge, K. K.; Boatz, J. A.; Elbert, S. T.; Gordon, M. S.; Jensen, J. H.; Koseki, S.; Matsunaga, N.; Nguyen, K. A.; Su, S. J.; Windus, T. L.; Dupuis, M.; Montgomery, J. A. *J. Comput. Chem.* **1993**, *14*, 1347.

(18) Nakano, H. *J. Chem. Phys*. **1993**, *99*, 7983−7992.

(19) MOLPRO is a package of ab initio programs written by H.-J. Werner and P. J. Knowles, with contributions from R. D. Amos, A. Bernhardsson, A. Berning, P. Celani, D. L. Cooper, M. J. O. Deegan, A. J. Dobbyn, F. Eckert, C. Hampel, G. Hetzer, T. Korona, R. Lindh, A. W. Lloyd, S. J. McNicholas, F. R. Manby, W. Meyer, M. E. Mura, A. Nicklass, P. Palmieri, R. Pitzer, G. Rauhut, M. Schütz, H. Stoll, A. J. Stone, R. Tarroni, and T. Thorsteinsson.

(20) Werner, H.-J. *Mol. Phys.* **1996**, *89*, 645.

(21) Stevens, W. J.; Basch, H.; Krauss, M.; Jasien, P. *Can. J. Chem.* **1992**, *70*, 612.

(22) Norman, J. H.; Staley, H. G.; Bell, W. E. *J. Phys. Chem.* **1967**, *71*, 3686.

(23) Norman, J. H.; Staley, H. G.; Bell, W. E. In *Advances in Chemistry Series*; Gould, R. F., Ed.; American Chemical Society: Washington, DC, 1968; Vol. 72, p 101.

(24) Lias, S. G.; Bartmess, J. E.; Liebman, J. F.; Holmes, J. L.; Levin, R. D.; Mallard, W. G. Gas-Phase Ion and Neutral Thermochemistry. In *J. Phys. Chem. Ref. Data, Suppl. 1* **1988**, *17*.

(25) Error estimated from ref 23.

(26) Zhang, X.-G.; Armentrout, P. B., University of Utah, personal communication; work in progress.

(27) Given the experimental uncertainties, thermal corrections between 0 and 298 K data appear negligible (see also: Kellogg, C. B.; Irikura, K. K. *J. Phys. Chem. A* **1999**, *103*, 1150). In this respect, the difference of 5 kcal/mol between the 0 and 298 K data for PtO in ref 24 may be a typo.

are observed. The rate constants for the consecutive $^{16}O/^{18}O$ exchanges show a 1.9:1 ratio, which is close to the 2:1 ratio expected for a statistical distribution of oxygen atoms.[8e] In contrast, hardly any $^{16}O/^{18}O$ exchange occurs with molecular oxygen $^{18}O_2$: the only product observed is a small amount of $[Pt,^{16}O,^{18}O]^+$ (possibly due to traces of $H_2{}^{18}O$ in the $^{18}O_2$ sample), and $[Pt,^{18}O_2]^+$ is absent even at long reaction times. As far as ion structure is concerned, the sequential $^{16}O/^{18}O$ exchanges with water suggest the existence of two equivalent oxygen atoms in $[Pt,O_2]^+$. Further, the near absence of $^{16}O/^{18}O$ exchange with $^{18}O_2$ disfavors the presence of an intact O−O bond, because replacement of a complete dioxygen unit is expected otherwise.[8a,c] These experimental data suggest, but cannot prove, a dioxide structure rather than a peroxo structure or a dioxygen complex; in other words, $OPtO^+$ is more plausible than $PtOO^+$ or $Pt(O_2)^+$.

Next, we turn our attention to the electron transfer observed with several substrates, to bracket the IE of the $[Pt,O_2]^+$ species formed in reaction 2. Electron transfer from the neutrals to $[Pt,O_2]^+$ to yield the corresponding cation radicals concomitant with neutral $[Pt,O_2]$ occurs almost exclusively with substrates such as benzene (IE = 9.2 eV) and ammonia (IE = 10.0 eV), whereas it amounts to about 40% of the products in the case of ethene (IE = 10.5 eV). Electron transfer is negligible (2%) with acetylene (IE = 11.7 eV) and absent with O_2 and Xe (both IE = 12.1 eV), as well as several other substrates having even larger IEs (H_2O, N_2O, CO, and Ar). These results suggest a rough bracket of 11.1 ± 0.6 eV. As this figure agrees reasonably well with IE(PtO_2) = 11.2 ± 0.3 eV derived from Knudsen-cell studies,[22,23] there appears no need to refine the bracket. The consistency of the IEs is noteworthy and suggests that the same species are sampled in both cases.[8e]

The ability of platinum to mediate O-atom transfer in the gas phase can be addressed by examination of reactions of $[Pt,O_2]^+$ with oxidizable substrates. Using molecular hydrogen as a neutral reagent, consecutive O-atom transfers from platinum to dihydrogen occur, reactions 3a and 4. In competition with reaction 3a, loss of hydroxyl radical is observed for the $[Pt,O_2]^+/H_2$ couple (reaction 3b). The $PtOH^+$ cation thus formed continues to react with hydrogen to afford platinum hydride as the final ionic product of this branch (reaction 5). The respective rate constants of reactions 3−5 are $k_3 = 1.1 \times 10^{-10}$ cm^3 molecules^{-1} s^{-1} (with k_{3a}:k_{3b} = 83:17), $k_4 = 5.0 \times 10^{-10}$ cm^3 molecules^{-1} s^{-1}, and $k_5 = 8.3 \times 10^{-10}$ cm^3 molecules^{-1} s^{-1}; note that the reduction of $[Pt,O_2]^+$ by H_2 is more than four times slower than that of PtO^+.

$$[Pt,O_2]^+ + H_2 \rightarrow PtO^+ + H_2O \quad (3a)$$

$$\rightarrow PtOH^+ + HO \quad (3b)$$

$$PtO^+ + H_2 \rightarrow Pt^+ + H_2O \quad (4)$$

$$PtOH^+ + H_2 \rightarrow PtH^+ + H_2O \quad (5)$$

When using D_2 instead of H_2, a similar sequence is observed. The intermolecular kinetic isotope effect is minor ($k_3(H_2)/k_3(D_2) \approx 1.3$), and the PtO^+:$PtOX^+$ (X = H, D) branching ratio is shifted only slightly from 83:17 for H_2 to 75:25 for D_2. The relatively small isotope effects on a reaction that involves H−H bond cleavage by definition suggests that other factors than the mere activation of the hydrogen−hydrogen bond contribute to the rate determining step, e.g., reorganization of the Pt−O bonds,

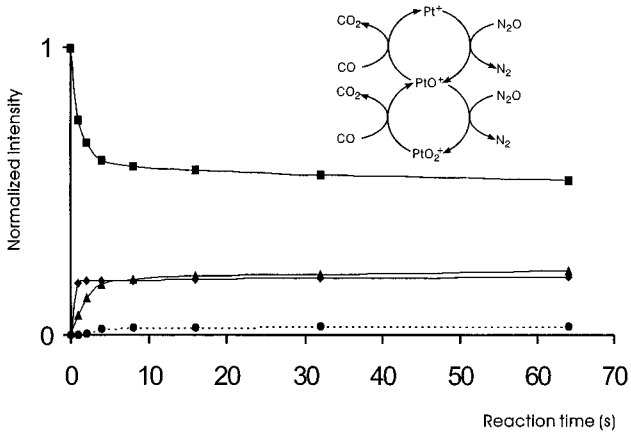

Figure 1. Temporal intensity profiles of $[Pt,O_2]^+$ (■), PtO^+ (◆), Pt^+ (▲), and the sum of all side products (●) when reacting mass-selected $[Pt,O_2]^+$ with a ca. 10:1 mixture of N_2O and CO (total pressure 10^{-7} mbar). The inset shows the catalytic cycles involved.

changes in spin multiplicities, etc.[28] We note in passing that the sequence of reactions 3b and 5 provides a rough bracket of 45 kcal/mol ≤ $D_0(Pt^+-OH)$ ≤ 77 kcal/mol for the so far unknown bond strength of the platinum−hydroxide cation.

In a similar manner, two successive reduction steps occur in the presence of carbon monoxide (reactions 6 and 7) with rate constants of $k_6 = 6.6 \times 10^{-10}$ cm^3 molecules^{-1} s^{-1} and $k_7 = 6.4 \times 10^{-10}$ cm^3 molecules^{-1} s^{-1}.

$$[Pt,O_2]^+ + CO \rightarrow PtO^+ + CO_2 \quad (6)$$

$$PtO^+ + CO \rightarrow Pt^+ + CO_2 \quad (7)$$

The clean reactions of the $[Pt,O_2]^+$/CO couple propose the realization of a catalytic cycle in the diluted gas phase.[29] Recently, a similar scenario for the oxidation of CO using N_2O has been proposed for anionic platinum clusters.[30] Upon treating $[Pt,O_2]^+$ with a mixture of CO and N_2O, quasistationary intensities of Pt^+, PtO^+, and $[Pt,O_2]^+$ are obtained (Figure 1); within experimental error, identical stationary intensities of Pt^+, PtO^+, and $[Pt,O_2]^+$ evolve when starting from Pt^+ and PtO^+, respectively. Hence, the combination of reactions 1, 2, 6, and 7 generates a sequence in which the gaseous platinum species effectively catalyze the conversion CO + $N_2O \rightarrow CO_2 + N_2$. The turnover number is basically limited by side reactions with background impurities; typical side products were $PtOH^+$, $PtO_2H_2^+$, $PtC_2H_4^+$, and $PtCH_2O^+$ whose abundances were subject to pronounced day-to-day fluctuations. In this particular case, the turnover number can simply be derived as the ratio of the initial rate constants and the apparent rate constant for the depletion of the catalytically active species Pt^+, PtO^+, and PtO_2^+ due to side reactions. In different runs turnover numbers ranging from 80 up to 300 were obtained.

Given the reactivity of $[Pt,O_2]^+$ toward H_2 and CO, it is not very surprising that methane is also activated efficiently by this cation. The rate constant $k(CH_4) = 2.5 \times 10^{-10}$ cm^3 molecules^{-1}

(28) See also: (a) Schröder, D.; Fiedler, A.; Ryan, M. F.; Schwarz, H. *J. Phys. Chem.* **1994**, *98*, 68. (b) Shaik, S.; Danovich, D.; Fiedler, A.; Schröder, D.; Schwarz, H. *Helv. Chim. Acta* **1995**, *78*, 1393. (c) Schröder, D.; Shaik, S.; Schwarz, H. *Acc. Chem. Res.* **2000**, *33*, 139.

(29) For other examples of gas-phase catalysis, see ref 7 in general; see also: (a) Kappes, M. M.; Staley, R. H. *J. Am. Chem. Soc.* **1981**, *103*, 1286. (b) Schnabel, P.; Weil, K. G.; Irion, M. P. *Angew. Chem.* **1992**, *104*, 633; *Angew. Chem., Int. Ed. Engl.* **1992**, *31*, 636. (c) Berg, C.; Kaiser, S.; Schindler, T.; Kronseder, C.; Niedner-Schatteburg, G.; Bondybey, V. E. *Chem. Phys. Lett.* **1994**, *231*, 139.

(30) Shi, Y.; Ervin, K. M. *J. Chem. Phys.* **1998**, *108*, 1757.

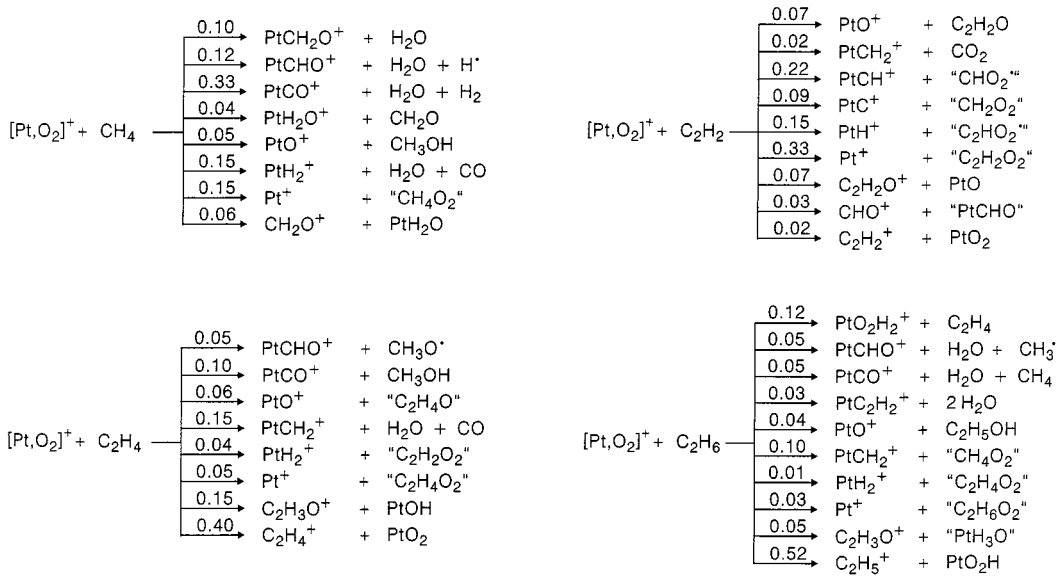

Figure 2. Products formed in the reactions of $[Pt,O_2]^+$ with the simple hydrocarbons methane, ethyne, ethene, and ethane. The assignment of the neutral product combinations, e.g. $H_2O + CO$ versus $H_2 + CO_2$, is not always unambiguous.

Table 1. Total Energies (in hartrees without ZPE) of the Local Minima on the $[Pt,O_2]^+$ Surface and Relevant Fragments Calculated at Several Levels of Theory

	B3LYP[a–c] BS I	B3LYP[a] BS II	B3LYP[a,d] BS III	BP86[a] BS III	MR-QDPT[a,e] BS IV	CASPT2[f] BS V	CASPT2[f] BS VI
$^2OPtO^+$	−269.05754	−269.15035	−269.36600	−269.51773	−268.82893	−268.34347	−268.58352
$^4OPtO^+$	−269.06177	−269.14011	−269.35405	−269.48732	−268.75189	−268.25070	−268.50221
$^2PtOO^+$	−269.09410	−269.14975	−269.37335	*g*	−268.78701[h]	−268.31257	−268.54322
$^4PtO^+$	−193.91773	−193.95693	−194.17572	−194.28266	−193.78956	−193.31026	−193.47396
$^3O_2$	−150.32548	−150.36908	−150.36908	−150.37910	−149.98637	−149.97490	−150.11425
$^2Pt^+$	−118.73549	−118.74049	−118.96423	−119.04139	−118.75610	−118.28878	−118.37557
^3O	−75.06657	−75.08557	−75.08557	−75.07542	−74.90776	−74.89709	−74.95893

[a] Geometry optimized. [b] Zero point energies (ZPEs) for $^2OPtO^+$, $^4OPtO^+$, $^2PtOO^+$, $^4PtO^+$, and $^3O_2$ (in hartrees): 0.00483, 0.00393, 0.00461, 0.00188, and 0.00374, respectively. [c] A quartet $^4PtOO^+$ ($^4A''$) complex was also found, $E_{tot} = -269.08651$. [d] ZPEs as in footnote *b*: 0.00494, 0.00397, 0.00462, 0.00182, and 0.00373, respectively. [e] No frequency analysis performed. [f] Single-point energies at MR-QDPT/BSIV geometries. [g] Not a minimum at this level (see text). [h] Manual geometry optimization, see theoretical section.

s^{-1} corresponds to about a quarter of the gas-kinetic collision rate. Formation of $PtO^+ + CH_3OH$ as side products as well as the occurrence of reaction 2 at thermal energies provide a crude bracket of 39 kcal/mol $< D_0(OPt^+-O) <$ 86 kcal/mol, which is consistent with the literature thermochemistry discussed above. Substrate activations close to collision rate occur for ethyne, ethene, and ethane ($k(C_2H_2) = 8.1 \times 10^{-10}$ cm^3 molecules^{-1} s^{-1}, $k(C_2H_4) = 8.7 \times 10^{-10}$ cm^3 molecules^{-1} s^{-1}, $k(C_2H_6) = 9.6 \times 10^{-10}$ cm^3 molecules^{-1} s^{-1}). Unfortunately, however, all these reactions lack selectivity and broad varieties of ionic and neutral products are formed (Figure 2). Moreover, several of the ionic products formed initially continue to react with the neutral substrates such that rather complex product patterns are obtained.

Ab Initio Study of $[Pt,O_2]^+$. Computational prediction of the properties of transition-metal species such as $[Pt,O_2]^+$ is highly challenging, in that accurate descriptions need to account for dynamical and nondynamical electron correlation as well as scalar and spin−orbit relativistic effects. Nevertheless, recent studies have shown that the use of density functional theory (DFT), especially the hybrid B3LYP functional in combination with adequate basis sets and relativistic effective core potentials (ECPs), leads to useful results for a wide range of problems in this field. Very recently, it has even been stated that "computational transition metal chemistry today is almost synonymous with DFT for medium-sized molecules".[31] Many studies, including some from our group,[32] have found this approach to be quite useful in unraveling the complex potential-energy surfaces of simple platinum compounds, especially when an approximate treatment of spin−orbit effects is included.[5]

Table 2. Optimized Bond Lengths (Å) and Angles (deg) of $[Pt,O_2]^+$ Isomers and the Fragments PtO^+ and O_2 for Comparison

		B3LYP/ BS I[a]	B3LYP/ BS III[b]	MR-QDPT/ BS IV[c]
$^4PtO^+$ ($^4\Sigma^-$)	r_{PtO}	1.755	1.746	1.736
$^2OPtO^+$ ($^2A_1/^2\Sigma_g^+$)	r_{PtO}	1.697	1.683	1.724
	α_{OPtO}	160.1	160.7	180.0
$^4OPtO^+$ ($^4B_2$)	r_{PtO}	1.774	1.760	1.770
	α_{OPtO}	110.2	112.6	114.6
$^2PtOO^+$ ($^2A''$)	r_{PtO}	2.049	2.016	1.95[d]
	r_{OO}	1.221	1.216	1.27[d]
	α_{PtOO}	118.7	117.3	107[d]
$^3O_2$ ($^3\Sigma_g^-$)	r_{OO}	1.215	1.208	1.243

[a] Geometry of $PtOO^+$ ($^4A'$) at the B3LYP/BS I level: $r_{PtO} = 2.145$ Å, $r_{OO} = 1.220$ Å, $\alpha_{PtOO} = 120.8$. [b] Unscaled harmonic vibrational computed at this level: $^4PtO^+$, 799 cm^{-1}; $^2OPtO^+$, 123 cm^{-1} (bend), 1007 cm^{-1} (symmetric stretch), 1037 cm^{-1} (asymmetric stretch); $^4OPtO^+$, 221 cm^{-1} (bend), 709 cm^{-1} (asymmetric stretch), 812 cm^{-1} (symmetric stretch); $^2PtOO^+$, 161 cm^{-1} (bend), 383 cm^{-1} (Pt−O stretch), 1486 cm^{-1} (O−O stretch), and $^3O_2$, 1637 cm^{-1}. Frequencies at the other DT levels were similar to these. [c] Frequency calculations were not performed at this level. [d] Manual geometry optimization, see theoretical section.

(31) Davidson, E. R. *Chem. Rev.* **2000**, *100*, 351.

(32) (a) Aschi, M.; Brönstrup, M.; Diefenbach, M.; Harvey, J. N.; Schröder, D.; Schwarz, H. *Angew. Chem.* **1998**, *110*, 858; *Angew. Chem., Int. Ed. Engl.* **1998**, *37*, 829. (b) Diefenbach, M.; Brönstrup, M.; Aschi, M.; Schröder, D.; Schwarz, H. *J. Am. Chem. Soc.* **1999**, *121*, 10614.

Table 3. Essential Energetics (kcal/mol) of the $[Pt,O_2]^+$ System at 0 K Calculated at Several Levels of Theory and Relevant Experimental Figures for Comparison

method[a]	B3LYPBS I[b]	B3LYPBS II	B3LYPBS III	BP86BS III	MR-QDPTBS IV	CASPT2BS V	CASPT2 BS VI	experiment
$D_0(Pt^+-O)$[c]	71.4	81.0	77.9	102.9	77.7	76.9	86.4	60[d]/75.2[e]
$D_0(OPt^+-O)$[f]	44.1	65.7	63.7	98.2	80.6	83.5	92.6	95[d]/71.0[e]
$D_0(Pt^+-O_2)$[g]	20.2	24.7	24.6	(/)[h]	27.4	30.1	33.0	
ΔE[i]	−23.1	0.2	−4.8	(/)[h]	26.1	19.2	25.1	
$D_0(O-O)$	118.3	121.9	121.9	140.9	104.9	111.1	120.9	118.0[d]

[a] Unless mentioned otherwise, approximate ZPE corrections are applied and taken from unscaled B3LYP/BSIII frequencies. For details on the level of geometry optimizations, see Table 1. [b] ZPE corrections from B3LYP/BSI calculations. [c] Previously calculated using B3LYP and PCI-80 to give $D_0(Pt^+-O) = 69.3$ and 72.3 kcal/mol, respectively, see ref 5. [d] Reference 24. [e] Reference 26. [f] Bond energy with respect to the dioxide structure $OPtO^+$. [g] Bond energy with respect to the peroxide structure $PtOO^+$. [h] $PtOO^+$ is not a minimum at this level. [i] Energy difference (E + ZPE) between $^2PtOO^+$ and $^2OPtO^+$.

Particularly noteworthy in the present context is the recent study of Andrews et al.,[33] where the chemistry of *neutral* $[Pt,O_2]$ was apparently successfully explored using B3LYP together with a polarized double-ζ basis.

It is against this background that we initially decided to explore the $[Pt,O_2]^+$ potential energy surfaces at the B3LYP level using the modest BS I (essentially LANL2DZ). At this level of theory, the doublet species $^2PtOO^+$ is predicted to be the most stable isomer of the $[Pt,O_2]^+$ system (Table 1). The bond lengths $r_{PtO} = 2.05$ Å and $r_{OO} = 1.22$ Å in conjunction with $\alpha_{PtOO} = 118.7°$ (Table 2) characterize this species as a superoxide. Alternatively, the structure can be regarded as a low-spin coupled, end-on dioxygen complex of $^2Pt^+$ and $^3O_2$. This bonding pattern is certainly suggested by the substantial spin contamination (typical values S^2 were 1.3−1.5, as against 0.75 expected for a pure doublet) of the doublet DFT "wave function", which indicates a considerable admixture of a quartet state of similar energy. Indeed, at the B3LYP/BSI level, a high-spin dioxygen complex $^4PtOO^+$ is only slightly higher in energy than the doublet. Further, $^2PtOO^+$ is predicted to lie 20.2 kcal/mol below the separated components, $^2Pt^+ + {}^3O_2$, which is a reasonable magnitude for an electrostatic interaction of a metal cation with dioxygen.[8a−c] The dioxo species $^2OPtO^+$ and $^4OPtO^+$ are some 20 kcal/mol higher in energy than $^2PtOO^+$ at this level of theory.

This result disagrees with the dioxide structure suggested by the experiments. Despite the fact that DFT results are often less basis-set dependent than conventional, wave function based ab initio techniques, we explored the use of the more flexible bases BS II and III. This does not significantly affect the description of PtO^+ (e.g., $D_0(Pt^+-O)$ is roughly constant, see Table 3), but leads to substantial changes of the relative stabilities of the $[Pt,O_2]^+$ species. Thus, the relative energy (ΔE_{rel}) of $^2PtOO^+$ and $^2OPtO^+$ ranges from −23.1 with BS I to 0.2 kcal/mol with BS II and −4.8 kcal/mol with BS III. In fact, from being much less stable than the superoxide, the dioxide becomes comparable in energy with the larger basis sets. However, the nature of the ground state is still ambiguous. Upon using another popular functional, BP86, together with BS III, the results are again different: there is no superoxide minimum, with optimization leading to the dioxo species. Overall, therefore, DFT results for this system are unreliable, and instead of any detailed discussion, they clearly demand benchmark calculations using wave function based ab initio methods.[34]

Exploratory computations using our initial method of choice, the very efficient single-reference CCSD(T) method, showed that it is not suitable for this problem, due to the substantial multireference character of the wave functions of several of the species investigated here. This was particularly the case for the dioxygen complexes of Pt^+ cation, but also for the $^2OPtO^+$ species, where near degeneracy in the π-orbitals seems to be responsible. We therefore turned to multireference methods. The MCSCF approach itself was found to give very poor results for the geometries of some of the species (e.g. $r(Pt^+-O)$ is predicted to be 1.9 Å), due to neglect of dynamical correlation. The first reliable method that is also reasonably computationally affordable is thus multireference perturbation theory to the second order (MR-PT2), of which we use the two different forms MC-QDPT and CASPT2. The MC-QDPT method with a medium-sized basis set (BS IV) was used for geometry optimization. Consistent energetics were obtained with CASPT2 computations using the similar-sized BS V. Our best results were obtained at the CASPT2 level with the larger BS VI at the MC-QDPT/BS IV optimized geometries (see Tables 1 and 2).

As far as electronic structure is concerned, a contrasting picture emerges from analysis of the MCSCF wave functions for the $PtOO^+$ ion and the other species. The superoxide shows only weak π-bonding between the two moieties, and could equally well be described as an ion−molecule complex with some additional bonding—in line with the doublet/quartet splitting near degeneracy observed in the DFT calculations. For the other compounds, i.e., $^4PtO^+$, $^2OPtO^+$, and $^4OPtO^+$, a similar pattern found to that in other transition-metal oxide cations emerges:[35] strong σ-bonding with electron donation to oxygen and much weaker π-overlap. This leads to substantial unpaired electron density on the metal, but also on oxygen, in all the species. To illustrate, the CASSCF Mulliken charge on platinum in $^2OPtO^+$ is of only +1.26. Compared to the formal oxidation state of +5, and even considering the inaccurate nature of Mulliken population analysis, this shows that the Pt−O "double bonds" are in fact quite weak and involve negligible transfer of electron density. It is conceivable that the poor results obtained here with density functional methods are due to the latter not being able to reproduce the very finely balanced interplay of correlation effects associated with these weak bonds.

Further, two important differences in geometry are noteworthy in comparing DFT and MR methods (Table 2). (i) DFT predicts $^2OPtO^+$ to be a slightly bent species, whereas at the MC-QDPT level, it is found to be linear. (ii) The MC-QDPT geometry of $^2PtOO^+$ is much more "superoxide-like" than the DFT structures, i.e., a notably shorter Pt−O bond along with an enlarged O−O distance and a stronger bending. It is noteworthy that the CASSCF geometry optimization leads to an even longer Pt−O bond, at ca. 2.2 Å, suggesting again that the combination of dynamic and nondynamic electron correlation is very important in weak bonding situations such as those found here.

(33) Bare, W. D.; Citra, A.; Chertihin, G. V.; Andrews, L. *J. Phys. Chem. A* **1999**, *103*, 5456.

(34) Koch, W.; Holthausen, M. C. *A Chemist's Guide to Density Functional Theory*; Wiley-VCH: Weinheim, 2000.

(35) See, for example: Kretzschmar, I.; Fiedler, A.; Harvey, J. N.; Schröder, D.; Schwarz, H. *J. Phys. Chem. A* **1997**, *101*, 6252.

Concerning energies, a far more consistent picture emerges from the MR-PT2 treatment compared to the DFT computations (Table 3). Specifically, the MR-QDPT/BS IV, CASPT2/BS V, and CASPT2/BS VI results are in reasonable agreement. Although even the largest basis set, BS VI, is certainly not converged, major changes (e.g. the ground-state assignment) are therefore not expected. On the basis of previous studies,[5] the effect of spin−orbit coupling on computed energetics is estimated to be of the order of maximum 5 kcal/mol. This is not large enough to affect the ground-state prediction given here.

CASPT2 calculations predict the doublet dioxide cation ^{2}-$OPtO^+$ to be the ground state and the global minimum of the $[Pt,O_2]^+$ system, with ΔE_{rel} compared to the next lowest structure, the superoxide $^2PtOO^+$, of ca. 25 kcal/mol. The CASPT2 results are reasonably consistent with experimental values of $D_0(Pt^+-O)$, $D_0(OPt^+-O)$, and $D_0(O-O)$ given in Table 3. However, the theoretical description is still incomplete. For example, the increases of $D_0(Pt^+-O)$ and $D_0(OPt^+-O)$ with BS IV to VI indicate that the dissociation behavior of PtO_n^+ is not yet described by these methods within chemical accuracy. Consequently, we refrain from deriving "best estimates" of the bond energies from the computational results. Obviously, the triatomic system $[Pt,O_2]^+$ poses a serious challenge to contemporary ab initio methods.

The most worrying aspect with regard to applied computational chemistry is, however, associated with another implication of this study. Thus, all methods—including DFT—agree reasonably well on the relative energetics of Pt^+, PtO^+, and even ^{2}-$PtOO^+$. In fact, in the absence of experimental results suggesting a dioxo structure for $[Pt,O_2]^+$, this reasonable agreement, also with literature thermochemistry and expected bond energies, would have suggested that DFT performs not too badly for the species of interest. This would have led to an incorrect assignment of the structure and properties of $[Pt,O_2]^+$. The benchmarking, however, clearly shows that the DFT methods simply fail to reach chemical relevance for this particular system. This observation should be taken as a warning to strenuously check the accuracy of DFT methods when these are applied to new types of bonding situations. Just as an example, the recent DFT study of a very closely related case, neutral $[Pt,O_2]$ isomers,[33] seems to suffer from similar shortcomings to those observed here. For example, the computed $D_0(OPt-O) = 87.4$ kcal/mol[33] is substantially lower than the value of 119 kcal/mol derived from the literature.[24] While noting this poor agreement concerning thermochemistry, we would, however, wish to underline that the main focus of the computational work in that paper was not on the energetics, but on the analysis of the vibrational frequencies and their isotopic shifts in particular. For these observables, good agreement with experiment was in fact reached on the basis of DFT computations, despite the poor results for bond energies and relative energies of isomers.

Conclusions

The $[Pt,O_2]^+$ cation is readily made by oxidation of bare Pt^+ using N_2O. $[Pt,O_2]^+$ is rather reactive and able to activate inert substrates such as H_2, CO, and CH_4. In the case of the $Pt^+/N_2O/CO$ system, this allows for a catalytic sequence in the gas phase in which the turnover number is basically limited by reactions with background contaminants. Unfortunately, however, already for methane oxidation the observed selectivity of O-atom transfer is rather low, and a manifold of product channels is accessed. Obviously, loss of selectivity in bond activation is the price to pay for the very high reactivity of $[Pt,O_2]^+$. In a more general context, one can conclude by extrapolation that platinum is suited to activate hydrocarbon substrates but likely to end up in combustion rather than selective, partial oxidation with molecular oxygen.

Our final computational results at the ab initio CASPT2 level are in reasonable agreement with the experimental data. In particular, they suggest that $[Pt,O_2]^+$ has an inserted, dioxo structure with sizable platinum−oxygen bond energies. While stating this positive outcome, we should not disguise the fact that in contrast to the experimental work, whose interpretation is more or less straightforward, our computational study of the $[Pt,O_2]^+$ system is rife with difficulties and misleading results. In particular, our initial computations using the popular B3LYP density functional lead to qualitatively incorrect results. In this respect, the $[Pt,O_2]^+$ system is a direct example in support of Koch's and Holthausen's recent warning not to accept DFT results in a too uncritical way.[34]

Acknowledgment. This work was gratefully supported by the Deutsche Forschungsgemeinschaft (SFB 546), the Volkswagen-Stiftung, the Fonds der Chemischen Industrie, the Bayer AG, and the Degussa-Hüls AG. We acknowledge Professor P. B. Armentrout for communicating unpublished results (ref 26) and Professor P. E. M. Siegbahn for providing us with a flexible platinum basis set. Further, we are indebted to the Konrad Zuse Zentrum for the generous allocation of computer time.

JA003138Q